Vol. 107: 211–221, 2014
doi: 10.3354/dao02685

DISEASES OF AQUATIC ORGANISMS
Dis Aquat Org

Published January 16

Henneguya cuniculator sp. nov., a parasite of spotted sorubim *Pseudoplatystoma corruscans* in the São Francisco Basin, Brazil

Juliana Naldoni[1], Antônio A. M. Maia[2,*], Marcia R. M. da Silva[2], Edson A. Adriano[1,3]

[1]Departamento de Biologia Animal da Universidade Estadual de Campinas (UNICAMP), Rua Monteiro Lobato, 255, CEP 13083-970, Campinas, Sao Paulo, Brazil

[2]Departamento de Ciências Básicas, Faculdade de Zootecnia e Engenharia de Alimentos, Universidade de São Paulo (USP), Rua Duque de Caxias Norte, 225, CEP 13635-900, Pirassununga, Sao Paulo, Brazil

[3]Departamento de Ciências Biológicas, Universidade Federal de São Paulo (UNIFESP), Rua Professor Artur Riedel, 275, Jardim Eldorado, CEP 09972-270, Diadema, Sao Paulo, Brazil

ABSTRACT: *Henneguya cuniculator* sp. nov. was found infecting spotted sorubim catfish *Pseudoplatystoma corruscans* from the São Francisco River, Minas Gerais, Brazil. The parasites form elongated plasmodia of up to 1 cm in length in the gill filaments. Mature spores were ellipsoidal from the frontal view, with total length of 29.4 ± 2.4 (mean ± SD, range 23.3–32.4) µm, body length of 12.1 ± 1.0 (10.0–14.7) µm, width of 4.8 ± 0.4 (4.0–5.9) µm, and tail length of 16.7 ± 2.0 (12.3–19.4) µm. From the lateral view, spores were biconvex, with thickness of 4.2 ± 0.7 (3.9–4.9) µm. The polar capsules were elongated and equal in size, 6.2 ± 0.3 (5.2–6.2) µm in length, and 1.8 ± 0.1 (1.4–1.9) µm in width. Ultrastructural analysis showed that the plasmodial wall had delicate projections towards the host tissue and a thin layer that prevented contact between the host cells and the parasite. In the ectoplasm, few mitochondria were observed, while generative cells, early stages of sporogenesis, and advanced spore development occurred in the plasmodial periphery, and more mature spores in internal regions. Histopathological analysis showed that plasmodia developed in the sub-epithelial connective tissue of gill filaments, causing compression of the adjacent tissues, deformation of gill filaments, and lamellar fusion. Phylogenetic analysis, based on 18S rDNA genes and using only *Henneguya*/*Myxobolus* species parasites of siluriform fish, showed grouping according to the fish family.

KEY WORDS: Myxozoa · *Pseudoplatystoma* · São Francisco River · 18S rDNA · Ultrastructure

INTRODUCTION

The spotted sorubim *Pseudoplatystoma corruscans* (Spix & Agassiz, 1829), popularly known in Brazil as 'pintado' or 'surubim,' is a catfish siluriform of the family Pimelodidae. It is found in the La Plata and São Francisco Basins of South America (Resende 2003). These carnivorous, migratory fish can reach up to 160 cm in length and 100 kg in weight (Froese & Pauly 2011), and due to the high quality of their meat, they play an important role in the fishing economy of the regions in which they are found (Campos 2005). *P. corruscans* is important for Brazilian aquaculture, as fingerlings created by crossbreeding of this species with *P. reticulatum* Eigenmann & Eigenmann, 1889 are reared in fish farms across the country (Naldoni et al. 2009). This hybrid fish is called 'pintado,' and its production in Brazilian fish farms

*Corresponding author: antomaia@usp.br

reached 2486 t in 2010 (MPA 2012). It is sold in the Brazilian market, and is also exported to several countries (Mar & Terra 2013).

The first report of a fish of the genus *Pseudoplatystoma* infected with a myxosporean was made by Eiras et al. (2009), who described *Henneguya corruscans* Eiras et al., 2009, infecting *P. corruscans* from the Paraná River. Since then, 5 other species have been described: *H. pseudoplatystoma* Naldoni et al., 2009, was found infecting hybrid pintado taken from fish farms in the states of São Paulo and Mato Grosso do Sul, and *H. eirasi* Naldoni et al., 2011, *H. multiplasmodialis* Adriano et al., 2012, *Henneguya m.* Carriero et al., 2013, and *Myxobolus flavus* Carriero et al., 2013, were found infecting both *P. corruscans* and *P. reticulatum* taken from natural environments in the Brazilian Pantanal wetland (Naldoni et al. 2009, 2011, Adriano et al. 2012, Carriero et al. 2013).

All myxozoan species described herein as occurring in *Pseudoplatystoma* spp. are from the La Plata Basin. We used morphologic, histologic, ultrastructural, and 18S rDNA sequencing data to describe a new *Henneguya* species that parasitizes the gill filaments of *Pseudoplatystoma corruscans* from natural environments in the São Francisco Basin.

MATERIALS AND METHODS

Ten specimens of *Pseudoplatystoma corruscans* (ranging from 56 to 93 cm in length) were collected from the São Francisco River (17° 12′ 8″ S, 44° 50′ 0″ W) in the municipality of Pirapora, state of Minas Gerais, Brazil. These samples were collected in July (n = 4) and December 2011 (n = 6). After capture, the fish were transported alive to the laboratory, where they were euthanized by benzocaine overdose (methodology approved by the ethics research committee of the Universidade Estadual de Campinas — proc. no. 2334-1), in accordance with Brazilian law (Federal Law No. 11.794, dated 8 October 2008 and Federal Decree No. 6899, dated 15 July 2009). The fish were then measured and necropsied. Plasmodia with mature spores were examined in fresh mounts with a light microscope. Morphological characterization of the spores was based on mature spores obtained from 3 different specimens. Measurements were performed on 30 spores using a computer equipped with Axivision 4.1 image capture software coupled to an Axioplan 2 Zeiss microscope. The dimensions of the spores are expressed as mean ± SD, in µm. Smears containing free spores were air-dried and stained with Giemsa solution and mounted in a low-viscosity mounting medium (CytosealTM) on permanent slides.

For histological analysis, fragments of infected organs were fixed in 10% buffered formalin and embedded in paraffin. Serial sections with a thickness of 4 µm were stained with hematoxylin-eosin.

For transmission electron microscopy, plasmodia were fixed in 2.5% glutaraldehyde in 0.1 M sodium cacodylate buffer (pH 7.4) for 12 h, washed in a glucose–saline solution for 2 h, and post-fixed in OsO_4. All of these processes were performed at 4°C. After dehydration using an acetone series, the material was embedded in EMbed 812 resin. Semithin sections were stained with toluidine blue solution and examined by light microscopy. Ultrathin sections, double stained with uranyl acetate and lead citrate, were examined in an LEO 906 electron microscope at 60 kV.

For molecular study, plasmodia were removed from the host tissue and fixed in absolute ethanol. The plasmodium content was collected in a 1.5 ml microcentrifuge tube and the DNA was extracted using the DNeasy® Blood & Tissue kit (Qiagen), following the manufacturer's instructions. The product was quantified in a NanoDrop 2000 spectrophotometer (Thermo Scientific) at 260 nm. PCR was carried out using a final volume of 25 µl, which contained 10 to 50 ng of extracted DNA, 1× *Taq* DNA polymerase buffer, 0.2 mmol of dNTP, 1.5 mmol of $MgCl_2$, 0.2 pmol of each primer, 0.25 µl (1.25 U) of *Taq* DNA polymerase (all reagents from Invitrogen by Life Technologies), and MilliQ (EMD Millipore) purified water in an Eppendorf AG 22331 Hamburg Thermocycler. Fragments of 1000 bp were amplified using the primers ERIB1+ACT1R (Barta et al. 1997), and fragments of 1200 bp were amplified using the primers MYXGEN+ERIB10 (Hallett & Diamant 2001, Diamant et al. 2004). An initial denaturation step at 95°C for 5 min was followed by 35 cycles of denaturation (95°C for 60 s), annealing (62°C for 60 s), and extension (72°C for 120 s); finishing with an extended elongation step at 72°C for 5 min. PCR products were electrophoresed in 1.0% agarose gel, stained with ethidium bromide, and analyzed in an FLA-3000 scanner (Fuji Photo Film). The size of the amplicons was estimated by comparison with the 1 kb DNA Ladder (Invitrogen by Life Technologies). Purified PCR products were sequenced using the same primer pair that was used in the amplification step, and another primer pair MC5-MC3 (Eszterbauer 2004) with the BigDye® Terminator v3.1 Cycle Sequencing kit (Applied Biosystems™) in an ABI 3730 DNA Analyzer (Applied Biosystems™). A stan-

dard nucleotide–nucleotide BLAST (blastn) search was conducted to verify the similarity of the sequence obtained in this study with other sequences available in the GenBank database (Altschul et al. 1997).

Phylogenetic analysis was performed using only myxosporean parasites of siluriforms available from GenBank. This included 13 sequences of *Henneguya* species and 2 sequences of *Myxobolus* species. *Ceratomyxa shasta* and *C. seriolae* were used as the outgroup. Nucleotide sequences were aligned using ClustalW inserted in BioEdit version 7.0.9.0 (Hall 1999). The Jmodeltest 0.1 program (Posada 2008) was used to choose the best evolution model of the sequences, and selected the GRT+G model. Nucleotide frequencies were estimated from the data (A = 0.2500, C = 0.2105, G = 0.2879, T = 0.2116). The 6 rates of nucleotide substitution were (AC) = 0.8263, (AG) = 2.2627, (AT) = 1.1733, (CG) = 0.6128, (CT) = 4.2650, (GT) = 1.0000, gamma shape = 0.3450. These parameters were used for maximum likelihood (ML) testing, which was conducted using PhyML 3.0 (Guindon et al. 2010). Bootstrap analysis (100 replicates) was employed to assess the relative robustness of the tree branches. The resulting tree was visualized with FigTree v1.3.1 (Rambaut 2008). Other alignment, including the species described in the present study and additional myxosporean parasites of pimelodids, was used to produce a pairwise similarity matrix using MEGA 5.0.

RESULTS

Eight of 10 (80%) specimens of *Pseudoplatystoma corruscans* taken from the São Francisco River had plasmodia of an unknown *Henneguya* species in the gill filaments.

Henneguya cuniculator sp. nov.

Description: The plasmodia were white and elongated, followed the line of the gill filaments, and measured up to 1 cm long (Fig. 1A). Histopathological analysis revealed that the plasmodia developed in the sub-epithelial connective tissue of the gill filaments, and expanded towards the lamellae. Development of the parasite resulted in compression of adjacent tissues, deformation of gill filaments and deformation and fusion of lamellae. Inflammatory infiltrate was not observed in the infection site (Figs. 2 & 3).

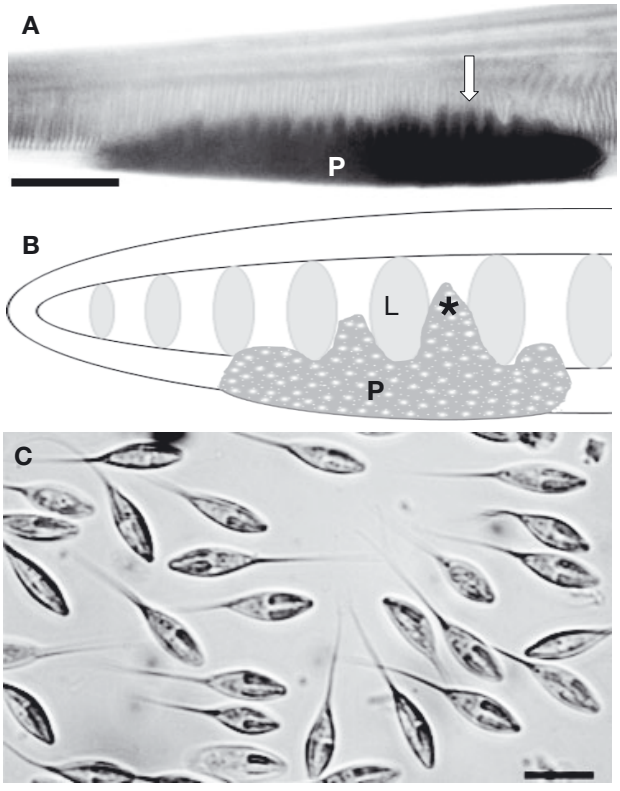

Fig. 1. *Henneguya cuniculator* sp. nov. infecting *Pseudoplatystoma corruscans*. (A) Formalin-fixed gill filament showing intrafilamental–epithelial plasmodium (P) growing towards the interlamellar region (arrow). Scale bar = 1000 µm. (B) Schematic drawing of a gill filament in frontal view showing the development of intrafilamental–epithelial plasmodium (P) growing towards the interlamellar region (*) and causing compression and deformation of the lamellae (L). (C) Mature fresh spores in frontal view. Scale bar = 10 µm

Mature spores were ellipsoidal from the frontal view, and had a total length of 29.4 ± 2.4 (23.3–32.4) µm, a body length of 12.1 ± 1.0 (10.0–14.7) µm, width of 4.8 ± 0.4 (4.0–5.9) µm, and a caudal process of 16.7 ± 2.0 (12.3–19.4) µm. From the lateral view, the spores were biconvex and had a thickness of 4.2 ± 0.7 (3.9–4.9) µm, while the valves were symmetrical. The polar capsules were elongated and equal in size, and had a length of 6.2 ± 0.3 (5.2–6.2) µm and a width of 1.8 ± 0.1 (1.4–1.9) µm (Table 1). The polar capsule occupied a little more than half of the body of the spore, and the anterior ends were adjacent (Fig. 1B). The polar filaments had 10 to 11 turns and were arranged perpendicularly to the longitudinal axis of the polar capsule (see Figs. 5B & 6).

Ultrastructure analysis revealed that the plasmodial wall was formed by a single membrane, and had numerous and extensive pinocytotic canals connecting the outside of the plasmodia to the ectoplasm zone (Fig. 4B). The plasmodial wall had delicate projec-

Table 1. *Henneguya* spp. Comparative data of *H. cuniculator* sp. nov. with other *Henneguya* species that are parasites of siluriform fishes. Spore dimensions, infection sites, and collection sites are given. LPC: length of polar capsules; WPC: width of polar capsules; NCF: number of coils of polar filaments; –: no data. All measurements are means ± SD and/or range, in µm

Species	Total length	Spore length	Spore width	Thick-ness	LPC	WPC	Tail length	NCF	Site of infection, host, and collection site	Source
H. adiposa	55.6 (40.7–65.8)	17.1 (14.7–20.5)	4.1 (3.4–4.6)	–	7.2 (5.8–8.3)	1.3 (0.9–1.9)	38.0 (23.2–48.8)	–	Adipose fin of *Ictalurus punctatus* (USA)	Minchew (1977)
H. ameiurensis	–	23.3	4.1	3.0	5.4	1.6	15.0–41.5	–	Barbels of *Ameiurus nebulosus* (USA)	Eiras (2002)
H. assuiti	45.5	12.3	5.1	–	6.0	1.54	–	9	Gills of *Clarias lazera* (Egypt)	Rabie et al. (2009)
H. basifilamentalis	–	14.0 ± 0.6 (13.0–15.0)	6.9 ± 0.5 (6.0–7.5)	2.8 ± 0.3 (4.0–5.0)	6.5 ± 0.8 (5.0–7.0) 5.1 ± 0.6 (4.0–5.6)	2.8 ± 0.4 (2.0–3.0) 2.6 ± 0.5 (1.3–2.0)	26.0–38.0	7	Basal crypts of hemibranchs of *Hemibagrus nemurus* (Malaysia)	Molnár et al. (2006)
H. bopeleti	44.5 (41.0–48.0)	17.2 (15.0–19.0)	6.3 (5.7–7.1)	–	8.0 (7–8.9)	2.0 (1.5–2.5)	27.4 (22.5–32.0)	7–9	Gills of *Chrysichthys nigrodogitatus* (Cameroon)	Eiras (2002)
H. camerounensis	16.7 (13.6–21.7)	10.2 (9.0–11.0)	4.4 (3.8–5.5)	–	5.3 (4.7–6.5)	1.3 (1.0–2.0)	–	–	Gills of *Synodontis batesi, Eutropius multitaeniatus*	Eiras (2002)
H. chrysichthyi	29.0 (27.0–32.0)	15.5 (13.7–16.0)	5.2 (4.6–6.3)	4.3 (4.0–4.5)	5.3 (4.6–5.7)	2.0 (1.6–2.2)	13.5 (10.0–15.0)	9–11	Gills of *Chrysichthys nigrodogitatus* (Nigeria)	Eiras (2002)
H. clariae	88.0 (45.0–107.0)	22.0 (17.5–28.5)	6.5 (5.5–8.5)	6.0 (5.5–7.5)	11.0 (5.5–13.5)	3.0 (2.5–3.5)	–	–	Gills of *Clarias lazera* (Nigeria)	Eiras (2002)
H. corruscans	27.6 (25.0–29.0)	14.3 (13.0–15.0)	5.0	–	6.8 (6.0–7.0)	2.0	13.7 (12.0–15.0)	5–6	Gills of *Pseudoplatystoma corruscans* (Brazil)	Eiras et al. (2009)
H. diversis	49.5 (40.0–62.0)	14.8 (13.5–16.5)	4.0 (3.2–5.0)	3.9 (3.0–4.5)	6.2 (6.0–7.5)	1.5 (1.0–2.0)	34.6 (25.0–47.0)	–	Base of barbels, pectoral fins, and along isthmus, liver, and kidney of *Ictalurus punctatus* (USA)	Minchew (1977)
H. eirasi	37.1±1.8	12.9±0.8	3.4±0.3	3.1±0.1	5.4±0.5	0.7±0.1	24.6±2.2	12–13	Gill filaments of *P. corruscans* and *P. fasciatum* (Brazil)	Naldoni et al. (2011)
H. exilis	60–70	18–20	4–5	3.0–3.5	8–9	1.0–1.5	15.0–41.5	–	Gills of *Ictalurus punctatus, Ameiurus melas, Ameiurus nebulosus* (USA)	Eiras (2002)
H. fusiformis	60.3 (59–61)	32.0 (29–33)	6.2 (5–7)	–	5.7 (5–6)	3.5 (3–4)	30.0 (28–31)	5–6	Gills of *Clarias anguilaris* (Chad)	Eiras (2002)
H. gurlei	60.9 (48.7–68.5)	18.2 (15.7–20.3)	5.4 (3.8–6.1)	3.2 (2.8–3.5)	5.9 (4.8–7.1)	1.2 (1.0–1.5)	41.1 (34.0–49.9)	–	Dorsal, pectoral, and anal fins of *Ameiurus nebulosus* (USA)	Iwanowicz et al. (2008)
H. ictaluri	–	23.9 (20.8–26.1)	6.0 (4.5–6.4)	–	8.1 (7.6–9.6)	2.5 (2.0–3.2)	63.0 (48.1–80.2)	–	Gills of *Ictalurus punctatus* (USA)	Eiras (2002)
H. latero-capsulata	32.7 (29.0–36.2)	14.7 (13.8–16.0)	4.3 (3.7–5.3)	3.8 (3.3–4.3)	4.8 (4.1–5.3)	2.6 (2.2–3.0)	18.0 (15.2–20.2)	–	Dermis of *Clarias lazera, H. bidorsalis,* hybrid (Israel)	Landsberg (1987)
H. longicauda	108.3 (91.0–127.0)	16.2 (14.0–17.5)	4.0 (3.4–4.5)	–	7.7 (7.0–8.5)	1.8 (1.5–2.0)	90.5 (75–110)	–	Gills of *Ictalurus punctatus* (USA)	Minchew (1977)

Table 1 (continued)

Species	Total length	Spore length	Spore width	Thickness	LPC	WPC	Tail length	NCF	Site of infection, host, and collection site	Source
H. maculosus	31.2	13.7±0.6	4.1±0.2	3.0±0.3	5.6±0.5	1.6±0.2	17.5±0.5	–	Gill filaments of *P. corruscans* (Brazil)	Carriero et al. (2013)
H. maculosus	33.0	13.3±0.7	4.4±0.4	3.5±0.4	5.2±0.6	1.6±0.2	19.7±0.6	–	Gill filaments of *P. reticulatum* (Brazil)	
H. multiplasmodialis	30.8±1.3	14.7±0.5	5.2±0.3	4.4±0.1	6.1±0.1	1.4±0.1	15.4±1.3	6–7	Large cysts in the gills of *P. corruscans* (Brazil)	Adriano et al. (2012)
H. multiplasmodialis	30.6±1.2	14.5±0.4	5.2±0.2	4.2±0.3	6.2±0.2	1.5±0.2	14.8±1.4	6–7	Large cysts in the gills of *P. fasciatum* (Brazil)	
H. mystusia	32.2 (27.0–40.0)	13.0 (12.0–15.0)	3.7 (3.0–4.0)	2.8 2.5–3.0)	5.04 (5.0–6.0)	1.2 (1.0–1.3)	19.3 (17.0–25.0)	–	Gills of *Mystus* sp. (India)	Eiras (2002)
H. nilotica	35.02–45.6	12.6–17.4	–	–	7.2–8.4	1.5–2.7	22–30	–	Secondary respiratory organ of *Clarias gariepinus* (*lazera*) (Egypt)	Rabie et al. (2009)
H. pellis	100.4 (79.0–124.0)	13.0 (11.0–14.5)	5.0 (4.5–5.2)	–	6.9 (5.5–8.5)	1.8 (1.5–2.0)	87.8 (66.0–112.0)	–	Skin of *Ictalurus furcatus* (USA)	Minchew (1977)
H. postexilis	52.0 (42.0–62.0)	15.0 (13.5–17.0)	3.4 (3.5–4.0)	3 (3.5–4.0)	6.6 (5.9–7.2)	1.5 (1.0–2.0)	37.0 (28.0–49.0)	–	Gills of *Ictalurus punctatus* (USA)	Minchew (1977)
H. pseudoplatystoma	33.2±1.9	10.4±0.6	3.4±0.4	–	3.3±0.4	1.0±0.4	22.7±1.7	6–7	Gills of hybrid pintado (Brazil)	Naldoni et al. (2009)
H. suprabranchiae	–	13 (11–14)	3 (2–5)	–	3 (2.5–5)	1 (1.5–4)	29 (27–30)	10–11	Suprabranchial organ of *Clarias gariepinus* (Egypt)	Landsberg (1987)
H. sutherlandi	65.9 (48.2–90.0)	15.4 (12.2–19.3)	5.5 (4.5–6.8)	–	6.1 (4.0–7.9)	1.7 (1.0–2.2)	50.5 (34.8–71.4)	6	Skin nodules of *Ictalurus punctatus* (USA)	Griffin et al. (2008)
H. cuniculator sp. nov.	29.4±2.4 (23.3–32.4)	12.1±1.0 (10.0–14.7)	4,8±0.4 (4.0–5.9)	4.2±0.7 (3.9–4.9)	6.2±0.3 (5.2–6.2)	1.8±0.1 (1.4–1.9)	16.7±2.0 (12.3–19.4)	10–11	Gill filaments of *P. corruscans* (Brazil)	This study

tions towards the host tissue and a thin layer, composed of fine granular material, which prevented contact between the host cells and the plasmodial wall (Fig. 4). A layer of fibrous material was observed throughout the periphery of the plasmodia, and in some cases, this layer of fibrous material was projected toward the interior of the plasmodia (Figs. 4A & 5A). Few mitochondria were observed underneath the ectoplasm. Below the ectoplasm, generative cells, early stages of sporogenesis, and advanced spore developmental stages were seen. Immature and mature spores were more prevalent internally (Fig. 4).

Molecular analysis, based on 18S rDNA genes from the spores of *Henneguya cuniculator* sp. nov. obtained from the gills of *Pseudoplatystoma corruscans,* resulted in a 1200 bp sequence that did not match any myxosporean species sequences available in GenBank. Analysis of the genetic divergence of the *Henneguya* species that parasitize *Pseudoplatystoma* spp. showed that the closest species to *H. cuniculator* sp. nov. was *H. multiplasmodialis* (1.7% divergence from that found infecting *P. reticulatum* and 1.8% from that found in *P. corruscans*), and the most distant was *H. maculosus* (13.1%) (Table 2).

Phylogenetic analysis, using only *Henneguya*/*Myxobolus* species parasites of siluriforms, formed 2 distinct strains. Clade A clustered 2 *Henneguya* species that parasitize fish of the Bagridae family. *M. cordeiroi*, a parasite of the pimelodid *Zungaru jahu,* appeared as a sister branch of the large clade B, which comprised *Henneguya*/*Myxobolus* parasites of pimelodids, ictalurids, and pangasids. Clade B further divided to form a sub-clade composed only of *Henneguya* species parasites of pimelodids of the genus *Pseudoplatystoma* and another composed of *Henneguya* species that parasitize ictalurids. *M. pangasii* and *M. hackyi* clustered together as a basal branch of the clade formed by parasites of ictalurids, and *M. flavus*, the unique *Myxobolus* species parasite of fish of the genus *Pseudoplatystoma*, appears as a basal branch of clade B. (Fig. 7).

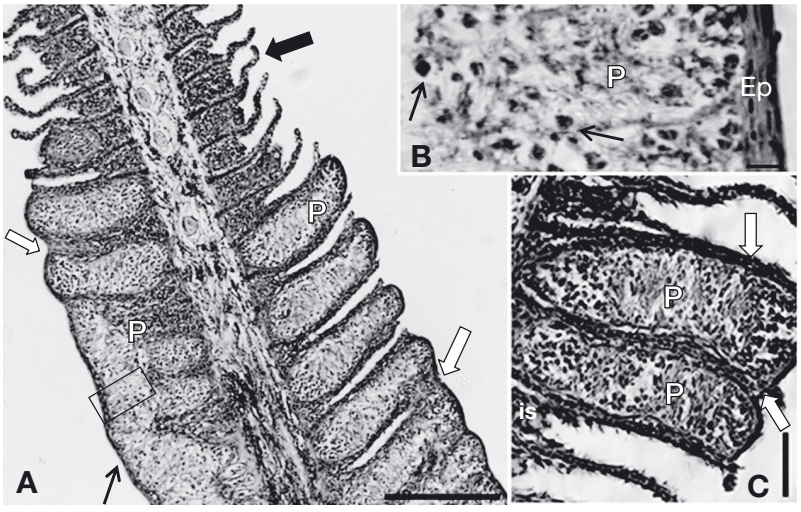

Fig. 2. *Pseudoplatystoma corruscans* infected by *Henneguya cuniculator* sp. nov. Light photomicrographs of histological sections of gill filaments. (A) Plasmodium (P) in sub-epithelial connective tissue (thin black arrow) occupying all area of the filament. Note normal lamellae (thick black arrow) and several deformed lamellae and lamellar fusion in areas affected by the growth of the plasmodium (white arrows). Scale bar = 200 µm. (B) Magnified section (rectangle) from (A); note the asynchronous process of sporogony inside the plasmodium (P), with young developmental stage spores (arrows) spread across all areas of the plasmodium. Ep: epithelium. Scale bar = 20 µm. (C) Detail of the development of plasmodium (P) growing towards the interlamellar regions occupying the entire interlamellar space (is) and causing deformation and compression of the lamellae (white arrows). Scale bar = 50 µm

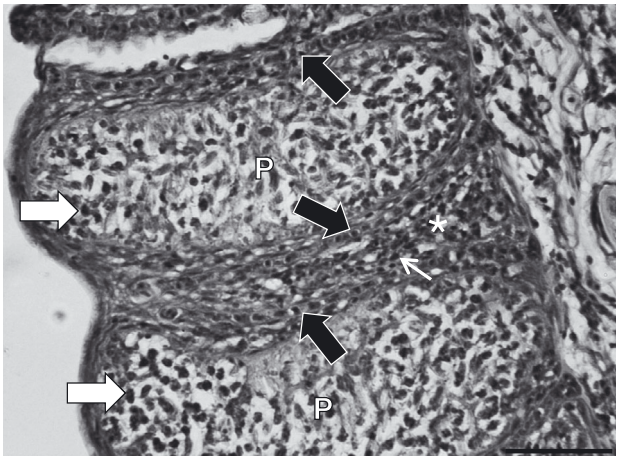

Fig. 3. *Pseudoplatystoma corruscans* infected by *Henneguya cuniculator* sp. nov. Light photomicrograph of histological section of gill filaments. Note deformation and compression of the interlamellar epithelium (*) with agglomerated nuclei of epithelial cells (thin white arrow), deformation of the lamellae (thick black arrows), and young developmental spores (thick white arrows) spread across all areas of the plasmodium (P). Scale bar = 50 µm

Prevalence: 8 of the 10 specimens (80%) of *Pseudoplatystoma corruscans* were infected.

Site of infection: gill filaments.

Host type: *Pseudoplatystoma corruscans*.

Specimens deposited: One slide containing spores fixed with methanol, stained with Giemsa stain solution, and mounted in a low-viscosity mounting medium, was deposited in the collection of the Museum of Natural History, Institute of Biology, Universidade Estadual de Campinas, state of São Paulo, Brazil (accession nos. ZUEC MYX 40 and ZUEC MYX 41). The 18S rDNA sequence was deposited in GenBank under accession number KF732840.

Locality: São Francisco River, municipality of Pirapora, state of Minas Gerais, Brazil.

Etymology: People born in the state of Minas Gerais are known in Portuguese as 'mineiros' ('miners') in reference to the widespread mining activity that developed in the region during the 17th and 18th centuries. 'Cuniculator' means 'miner' in Latin. Therefore the specific name is related to the place where the parasite was found.

DISCUSSION

Six myxosporeans have been found to infect the gills of fish of the genus *Pseudoplatystoma*. *Henneguya pseudoplatystoma* was found infecting gill filaments of pintado hybrids from fish farms, causing stretching and deformation of these structures, leading to a reduction of the functional area of the epithelium (Naldoni et al. 2009). *H. eirasi* was found parasitizing gill filaments of *P. corruscans* and *P. reticulatum* from natural environments in the Brazilian Pantanal wetland, and produced only slight compression of the adjacent tissues (Naldoni et al. 2011). *H. corruscans* was described infecting the gill lamellae from *P. corruscans* from natural environments in the Paraná River and caused hypertrophy of the infected lamella (Eiras et al. 2009). *H. multiplasmodialis* was found forming large plasmodia on the surface of the gills of *P. corruscans* and *P. reticulatum* from the Brazilian Pantanal wetland. The plasmodia of this species were arranged unusually, being externally enveloped by a stratified epithelium composed of several cell types, with a predominance of mucus

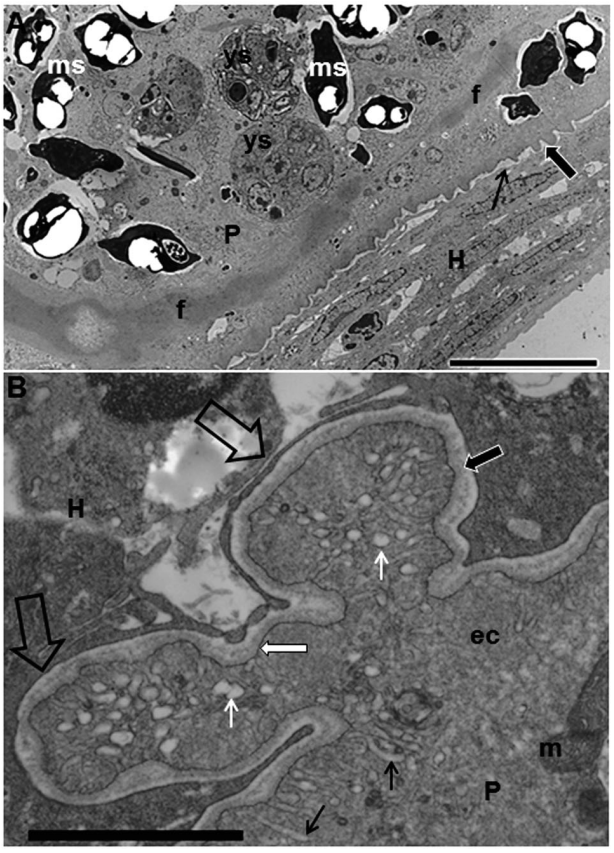

Fig. 4. *Pseudoplatystoma corruscans* infected by *Henneguya cuniculator* sp. nov. Electron micrograph of gill filaments. (A) Host–parasite interface showing host tissue (H) separated from plasmodium by a layer of fine granular material (thin arrow) and delicate projections of the plasmodial wall (thick arrow). Note the presence of a layer of fibrous material (f) in the periphery of the plasmodium, young sporoblasts (ys), and mature spores (ms). Scale bar = 10 µm. (B) Amplified portion of the host–parasite interface showing the projection of plasmodial expansion (empty arrows) toward the host tissue (H) and a layer of granular material (thick black arrow) separating the plasmodial (P) from the host cells. Note the single plasmodial membrane (thick white arrow) with numerous pinocytic channels (thin black arrows) toward the ectoplasm zone (ec) and ending in pinocytic vesicles (thin white arrows). Scale bar = 2 µm

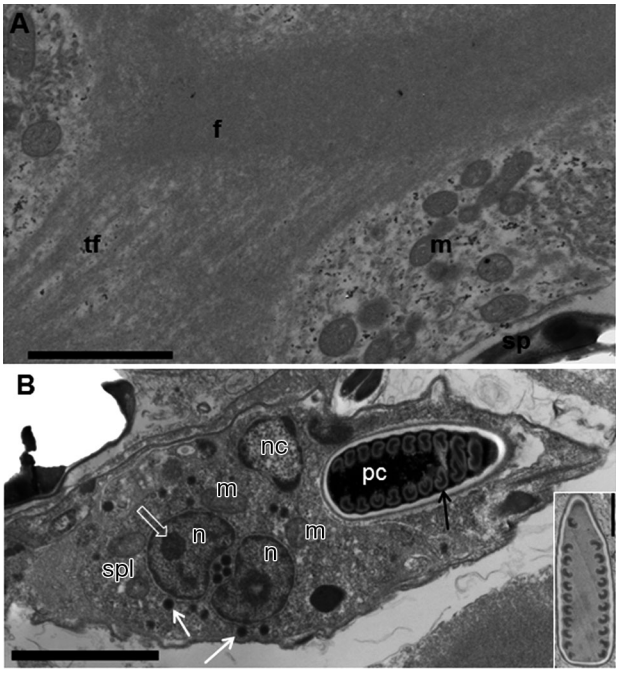

Fig. 5. *Henneguya cuniculator* sp. nov. infecting *Pseudoplatystoma corruscans*. Electron micrograph of plasmodium of *H. cuniculator* sp. nov. parasitizing gill filaments of *P. corruscans*. (A) Details of layer of fibrous material (f) of the periphery of the plasmodia showing thin fibriles (tf), mitochondria (m), and part of a spore. Scale bar = 5 µm. (B) Longitudinal section of a young spore showing sporoplasm binucleate with nucleoli (n, empty arrow), sporoplasmosomes (spl, white arrows), and several mitochondria (m); polar capsule (pc) with polar filaments (black arrow) and nucleus of the capsulogenic cell (nc). Scale bar = 2.5 µm. On the right is a longitudinal section of a whole polar capsule showing the number of turns of the polar filament. Scale bar = 1 µm

Fig. 6. *Henneguya cuniculator* sp. nov. Schematic representation of the mature spore of *H. cuniculator* sp. nov., a parasite of *Pseudoplatystoma corruscans*. Scale bar = 10 µm

and club cells. Internally, the plasmodia were composed of a network of septa formed by connective tissue, dividing the plasmodium into compartments, with inflammatory infiltrate in the tissue surrounding the plasmodium, as well as in the septa (Adriano et al. 2012). *H. maculosus* was found in the gill filaments and *M. flavus* in the gill arch (Carriero et al. 2013) of fish from the Brazilian Pantanal wetland, but histological analysis was not performed. In the species analyzed in the present study, histological analysis revealed the development of the plasmodia in the sub-epithelial connective tissue of the gill filaments, producing compression of the adjacent tissues, deformation of the gill filaments, and lamellar fusion, leading to the reduction of the functional epithelium area in a similar manner to *H. pseudoplatystoma* (Naldoni et al. 2009). However, as observed for *H. corruscans*, *H. pseudoplatystoma*, and *H. eirasi*, inflammatory infiltrate was not found at the infection site.

Ultrastructural analysis of the host–parasite interface of *Henneguya cuniculator* sp. nov. showed a thin

Table 2. *Henneguya* spp. Pairwise genetic identity of the 18S rRNA gene of *H. cuniculator* sp. nov. and related *Henneguya* species that are parasites of fish of the genus *Pseudoplatystoma*. The area above the diagonal shows nucleotide differences in relation to the number of bases compared. The area below the diagonal shows % pairwise distance identity

	Species	1	2	3	4	5	6	7	8
1	*H. cuniculator* sp. nov.	–	18/1030	22/1214	53/1215	50/1214	107/915	136/1222	156/1206
2	*H. multiplasmodialis* (*P. reticulatum*)	1.7	–	11/1316	82/1315	85/1315	184/1329	208/1340	213/1330
3	*H. multiplasmodialis* (*P. corruscans*)	1.8	0.8	–	109/1559	109/1562	187/1210	241/1592	268/1507
4	*H. corruscans* (*P. corruscans*)	4.2	6.3	7.0	–	44/1895	193/1206	259/1938	273/1504
5	*H. corruscans* (*P. reticulatum*)	4.1	6.5	7.0	2.3	–	202/1206	266/1924	269/1505
6	*H. eirasi* (*P. reticulatum*)	11.8	15.6	15.9	16.4	17.1	–	111/1209	116/1209
7	*H. maculosus* (*P. corruscans*)	11.3	15.9	15.5	13.7	14.1	9.2	–	29/1496
8	*H. maculosus* (*P. reticulatum*)	13.1	16.4	18.0	18.4	18.1	9.7	1.9	–

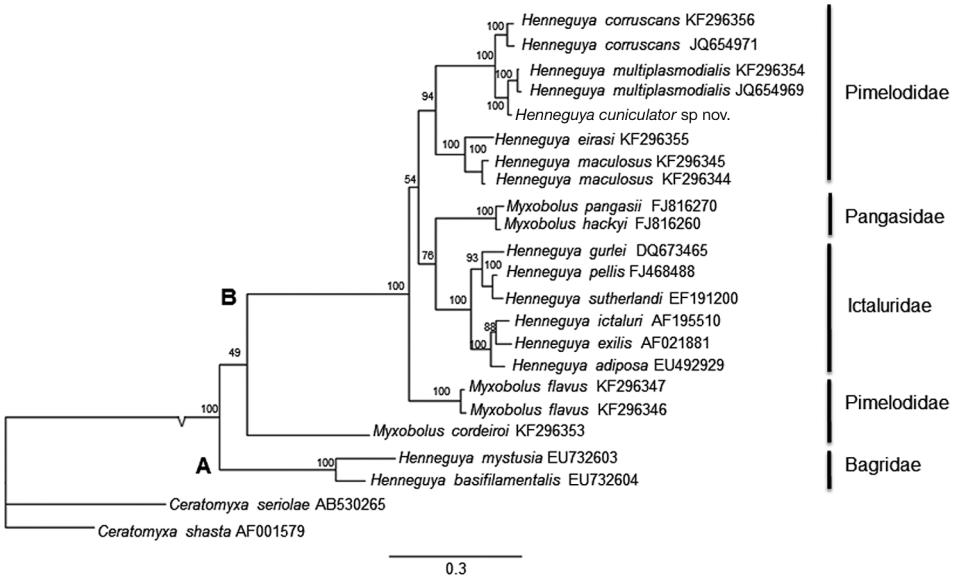

Fig. 7. *Henneguya* spp. and *Myxobolus* spp. Maximum likelihood tree showing relationship between *H. cuniculator* sp. nov. and other *Henneguya* and *Myxobolus* species that are parasites of siluriform fish based on the 18S rDNA gene. Numbers above nodes indicate bootstrap confidence levels; A and B mark branch points defining clades A and B

layer of fine granular material preventing contact between the plasmodium and the host tissue, while numerous pinocyte canals connected the outside of the plasmodia to the ectoplasm zone, demonstrating the intense nutritional activity of the plasmodium. The plasmodial wall of *H. cuniculator* sp. nov., which was comprised of a single membrane, also presented delicate projections towards the host tissue, seemingly seeking increased surface contact with the host tissue, a mechanism related to nutritional activity, as also observed by Naldoni et al. (2009) and El-Mansy & Bashtar (2002). The sporogenesis process of *H. cuniculator* sp. nov. was similar to those observed in other species of *Henneguya* (Matos et al. 2005, Ali et al. 2007, Abdel-Ghaffar et al. 2008, Azevedo et al. 2008, Naldoni et al. 2009, 2011, Barassa et al. 2012). However, the plasmodia of *H. cuniculator* sp. nov. presented a conspicuous layer of slightly electron-dense fibrous material spreading throughout the periphery. This material is similar to that observed in the periphery of *H. pseudoplatystoma* and *H. eirasi* (Naldoni et al. 2009, 2011). According to Naldoni et al. (2009), this electron-dense fibrous material corresponds to actin filaments and may play a role in the support of the plasmodium. Fibrous material resembling aggregated actin anchoring the mural cells of the presporogonic cells of the malacosporean *Tetracapsuloides bryosalmonae* was also reported by Morris & Adams (2007). The presence of microfilaments in the developmental stages of myxosporeans was also reported by Casal et al. (1997), who identified myosin filaments occupying the space of pericyte cells of *H. striolata* Casal et al. 1997.

The morphologic and morphometric characteristics of *Henneguya cuniculator* sp. nov. were compared with those of all *Henneguya* spp. that parasitize siluriform fish (Eiras 2002, Rabie et al. 2009, Eiras & Adriano 2012). Spores of the species *H. multiplasmodialis, H. maculosus, H. corruscans*, *H. suprabranchiae* Landsberg, 1987, and *H. nilotica* Marwan, 1998 had a higher morphometric and morphologic resemblance to those of *H. cuniculator* sp. nov. Nevertheless, a

small number of subtle morphologic differences were observed, such as spore body length (12.1 µm for *H. cuniculator* sp. nov.; 13.3 and 13.7 µm for *H. maculosus*, 14.5 and 14.7 µm for *H. multiplasmodialis*, and 14.3 µm for *H. corruscans*) and the number of turns of the polar filaments (10 to 11 turns in *H. cuniculator* sp. nov., 6 to 7 turns in *H. multiplasmodialis* and *H. maculosus*, and 5 to 6 turns in *H. corruscans*). Differences may also be observed in the length of the polar capsules (6.2 µm for *H. cuniculator* sp. nov. and 3 µm for *H. suprabranchiae*) and in tail length (16.7 µm for *H. cuniculator* sp. nov; 13.7 µm for *H. corruscans*; 22 to 30 µm for *H. nilotica*, and 29 µm for *H. suprabranchiae*; detailed morphometric data are displayed in Table 1). Other important differences observed relate to the host, location of infection sites, and appearance of the plasmodia, which were small and in the gill lamellae in case of *H. corruscans* (Eiras et al. 2009) and large and on the gill surface in case of *H. multiplasmodialis* (Adriano et al. 2012), while the plasmodia of *H. cuniculator* sp. nov. were located in the internal areas of the gill filaments. *H. suprabranchiae* infects the hyaline cartilage of the suprabranchial organ of *Clarias gariepinus* (Burchell, 1822) (El-Mansy & Bashtar 2002) and *H. nilotica* forms spherical plasmodia in the tips of the suprabranchial organ of *C. lazera* Valenciennes, 1840 (junior synonym of *C. gariepinus*) (Rabie et al. 2009).

Geography should also be considered. *Pseudoplatystoma corruscans* is known to inhabit rivers from the La Plata and São Francisco basins (Resende 2003). However, in phylogenetic studies of *Pseudoplatystoma* species, based on analysis of cytochrome *b* mtDNA sequences, Carvalho-Costa et al. (2011) showed the existence of geographically distinct clades for *P. corruscans*, with the samples from the São Francisco and La Plata Basins being clearly separated. According to those authors, *P. corruscans* haplotypes from the São Francisco Basin are on average 1.5% divergent from the populations from the La Plata Basin. The authors also pointed out that these genetic differences suggest a substantial period of evolutionary divergence and speculated that such divergence may be related to reproductive isolation, since these populations have been geographically separated for a considerable time. In this same way, geography may also contribute to the divergence of these parasites, as *Henneguya cuniculator* sp. nov. infects *P. corruscans* from the São Francisco Basin, while *H. multiplasmodialis, H. maculosus*, and *H. corruscans* were described in *P. corruscans* and *P. reticulatum* taken from rivers from the La Plata Basin.

There is no exact value that defines at what point a difference in the 18S rDNA genes of a myxozoan species should be considered as intra- or interspecific variation (Gunter & Adlard 2009). However, according to Cech et al. (2012), identity values close to 100% undoubtedly indicate that the 2 species are identical, but a 98–99% sequence identity makes it difficult to decide whether a single or multiple species are being considered. The comparison of the 18S rDNA gene sequences from *Henneguya cuniculator* sp. nov. with *H. multiplasmodialis* in *Pseudoplatystoma* spp. shows genetic divergence of 1.7–1.8% (Table 2). The small genetic divergence observed between *H. cuniculator* sp. nov. and *H. multiplasmodialis* is not robust enough to be defined as an interspecific variation and would not by itself be strong enough to separate these 2 *Henneguya* species. On the other hand, this genetic divergence, when added to other data such as site of parasite development, the histologic appearance of the plasmodia, differences in spore characteristics (smaller spore body length and higher number of polar filaments turns in *H. cuniculator* sp. nov.), strongly support the separation of these species. Another important aspect to be considered here is the extended period of geographical isolation of the La Plata and São Francisco Basins, which can play a decisive role in genetic divergence, as observed by Carvalho-Costa et al. (2011) in the *P. corruscans* populations from these 2 basins. Based on such morphologic, molecular, and geographic arguments, we believe that there is enough evidence to support the creation of new species.

The phylogenetic studies of the sequences of *Henneguya* and *Myxobolus* available in the GenBank database illustrate a general tendency to group according to the taxonomic affinities of the host fish (Ferguson et al. 2008, Naldoni et al. 2011, Adriano et al. 2012, Carriero et al. 2013). Thus, in the present study, phylogenetic analysis was performed only for *Henneguya*/*Myxobolus* species that are parasites of siluriform fish. The results showed that the grouping of *Henneguya*/*Myxobolus* exactly followed the family of host fish, corroborating the hypothesis of a notably close relationship between the evolution of *Henneguya*/*Myxobolus* parasites and their hosts.

Acknowledgements. We thank J. L. Bartholomew (Center for Fish Disease Research of the Department of Microbiology, Oregon State University) for undertaking a critical reading of the manuscript and the anonymous reviewers for their suggestions, which helped to improve this article. Financial support was received from CNPq (Proc. no. 472747/2012-6). J.N. was supported by a FAPESP scholarship (Proc. no. 2011/10738-1).

LITERATURE CITED

Abdel-Ghaffar F, Abdel-Baki AS, Bayoumy EM, Bashtar AR and others (2008) Light and electron microscopic study on *Henneguya suprabranchiae* Landsberg, 1987 (Myxozoa: Myxosporea) infecting *Oreochromis niloticus*, a new host record. Parasitol Res 103:609–617

Adriano EA, Carriero MM, Maia AAM, Silva MRM, Naldoni J, Ceccarelli OS, Arana S (2012) Phylogenetic and host–parasite relationship analysis of *Henneguya multiplasmodialis* n. sp. infecting *Pseudoplatystoma* spp. in Brazilian Pantanal wetland. Vet Parasitol 185:110–120

Ali MA, Abdel-Baki AS, Sakran Th, Entzeroth R, Abdel-Ghaffar F (2007) *Myxobolus lubati* n. sp. (Myxosporea: Myxobolidae), a new parasite of haffara seabream *Rhabdosargus haffara* (Forsskal, 1775), Red Sea, Egypt: a light and transmission electron microscopy. Parasitol Res 100: 819–827

Altschul SF, Madden TL, Schaffer AA, Zhang J, Zhang Z, Miller W, Lipman DJ (1997) Gapped BLAST and PSI-BLAST: a new generation of protein database search programs. Nucleic Acids Res 25:3389–3402

Azevedo C, Casal G, Matos P, Matos E (2008) A new species of Myxozoa, *Henneguya rondoni* n. sp. (Myxozoa), from the peripheral nervous system of the Amazonian fish, *Gymnorhamphichthys rondoni* (Teleostei). J Eukaryot Microbiol 55:229–234

Barassa B, Adriano EA, Cordeiro NS, Ceccarelli PS (2012) Morphology and host–parasite interaction of *Henneguya azevedoi* n. sp., parasite of gills of *Leporinus obtusidens* from Mogi-Guaçu River, Brazil. Parasitol Res 110: 887–894

Barta JR, Martin DS, Liberato PA, Dashkevicz M and others (1997) Phylogenetic relationships among eight *Eimeria* species infecting domestic fowl inferred using complete small subunit ribosomal DNA sequences. J Parasitol 83: 262–271

Campos JL (2005) O cultivo do pintado, *Pseudoplatystoma corruscans* (Spix & Agassiz 1829). In: Baldisserotto B, Gomes LC (eds) Espécies nativas para piscicultura no Brasil. UFSM, Santa Maria, p 327–343

Carriero MM, Adriano EA, Silva MRM, Ceccarelli PS, Maia AAM (2013) Molecular phylogeny of the *Myxobolus* and *Henneguya* genera with several new South American species. PLoS ONE 8:e73713

Carvalho-Costa LF, Piorski NM, Willis SC, Galetti PM Jr, Ortí G (2011) Molecular systematics of the neotropical shovelnose catfish genus *Pseudoplatystoma* Bleeker 1862 based on nuclear and mtDNA markers. Mol Phylogenet Evol 59:177–194

Casal G, Matos E, Azevedo C (1997) Some ultrastructural aspects of *Henneguya striolata* sp. nov. (Myxozoa, Myxosporea), a parasite of the Amazonian fish *Serrasalmus striolatus.* Parasitol Res 83:93–95

Cech G, Molnár K, Székely C (2012) Molecular genetic studies on morphologically indistinguishable *Myxobolus* spp. infecting cyprinid fishes, with the description of three new species, *M. alvarezae* sp. nov., *M. sitjae* sp. nov. and *M. eirasianus* sp. nov. Acta Parasitol 57:354–366

Diamant A, Whipps CM, Kent ML (2004) A new species of *Sphaeromyxa* (Myxosporea: Sphaeromyxina: Sphaeromyxidae) in devil firefish, *Pterois miles* (Scorpaenidae), from the northern Red Sea: morphology, ultrastructure, and phylogeny. J Parasitol 90:1434–1442

Eiras JC (2002) Synopsis of the species of the genus *Henneguya* Thelohan, 1892 (Myxozoa: Myxosporea: Myxobolidae). Syst Parasitol 52:43–54

Eiras JC, Adriano EA (2012) A checklist of new species of *Henneguya* Thelohán, 1892 (Myxozoa: Myxosporea, Myxobolidae) described between 2002 and 2012. Syst Parasitol 83:95–104

Eiras JC, Takemoto RM, Pavanelli GC (2009) *Henneguya corruscans* n. sp. (Myxozoa, Myxosporea, Myxobolidae), a parasite of *Pseudoplatystoma corruscans* (Osteichthyes, Pimelodidae) from the Parana River, Brazil: a morphological and morphometric study. Vet Parasitol 159:154–158

El-Mansy A, Bashtar AR (2002) Histopathological and ultrastructural studies of *Henneguya suprabranchiae* Landsberg 1987 (Myxosporea; Myxobolidae) parasitizing the suprobranchial organ of the freshwater catfish *Clarias gariepinus* Burchell 1822 in Egypt. Parasitol Res 88: 617–626

Eszterbauer E (2004) Genetic relationship among gill-infecting *Myxobolus* species (Myxosporea) of cyprinids: molecular evidence of importance of tissue-specificity. Dis Aquat Org 58:35–40

Ferguson JA, Atkinson SD, Whipps CM, Kent ML (2008) Molecular and morphological analysis of *Myxobolus* spp. of salmonid fishes with the description of a new *Myxobolus* species. J Parasitol 94:1322–1334

Froese R, Pauly D (2011) FishBase. www.fishbase.org (accessed on 5 March 2013)

Griffin MJ, Pote LM, Wise DJ, Greenway TE, Mauel MJ, Camus AC (2008) A novel *Henneguya* species from channel catfish described by morphological, histological, and molecular characterization. J Aquat Anim Health 20:127–135

Guindon S, Dufayard JF, Lefort V, Anisimova M, Hordijk W, Gascuel O (2010) New algorithms and methods to estimate maximum-likelihood phylogenies: assessing the performance of PhyML 3.0. Syst Biol 59:307–321

Gunter NL, Adlard RD (2009) Seven new species of *Ceratomyxa* Thelohan, 1892 (Myxozoa) from the gall-bladders of serranid fishes from the Great Barrier Reef, Australia. Syst Parasitol 73:1–11

Hall TA (1999) BioEdit: A user-friendly biological sequence alignment editor and analysis program for Windows 95/98/NT. Nucleic Acids Symp Ser 41:95–98

Hallett SL, Diamant A (2001) Ultrastructure and small-subunit ribosomal DNA sequence of *Henneguya lesteri* n. sp. (Myxosporea), a parasite of sand whiting *Sillago analis* (Sillaginidae) from the coast of Queensland, Australia. Dis Aquat Org 46:197–212

Iwanowicz LR, Iwanowicz DD, Pote LM, Blazer VS, Schill WB (2008) Morphology and 18S rDNA of *Henneguya gurlei* (Myxosporea) from *Ameiurus nebulosus* (Siluriformes) in North Carolina. J Parasitol 94:46–57

Landsberg JH (1987) Myxosporean parasites of the catfish, *Clarias lazera* (Valenciennes). Syst Parasitol 9:73–81

Mar & Terra (2013) Our production process: logistics and transportation. Available at www. mareterra.com.br/site 2013/empresa.asp?lang=in (accessed on 5 March 2013)

Matos E, Tajdari J, Azevedo C (2005) Ultrastructural studies of *Henneguya rhamdia* n. sp. (Myxozoa) a parasite from the Amazon teleost fish, *Rhamdia quelen* (Pimelodidae). J Eukaryot Microbiol 52:532–537

Minchew CD (1977) Five new species of *Henneguya* (Protozoa: Myxosporida) from ictalurid fish. J Protozool 24: 213–220

Molnár K, Székely C, Mohamed K, Shaharom-Harrison F (2006) Myxozoan pathogens in cultured Malaysian

fishes. I. Myxozoan infections of the sutchi catfish *Pangasius hypophthalmus* in freshwater cage cultures. Dis Aquat Org 68:209–218

Morris DJ, Adams A (2007) Sacculogenesis and sporogony of *Tetracapsuloides bryosalmonae* (Myxozoa: Malacosporea) within the bryozoan host *Fredericella sultana* (Bryozoa: Phylactolaemata). Parasitol Res 100:983–992

MPA (Ministério da Pesca e Aqüicultura) (2012) Boletim estatístico da pesca e aquicultura. MPA, Brasília

Naldoni J, Arana S, Maia AAM, Ceccarelli PS and others (2009) *Henneguya pseudoplatystom*a n. sp. causing reduction in epithelial area of gills in the farmed pintado, a South American catfish: histopathology and ultrastructure. Vet Parasitol 166:52–59

Naldoni J, Arana S, Maia AAM, Silva MRM and others (2011) Host–parasite–environment relationship, morphology and molecular analysis of *Henneguya eirasi* n. sp. parasite of two wild *Pseudoplatystoma* ssp. in Pantanal Wetland, Brazil. Vet Parasitol 177:247–255

Posada D (2008) JModelTest: phylogenetic model averaging. Mol Biol Evol 25:1253–1256

Rabie SA, Mohammed NI, Hussein AA, Hussein NM (2009) The infection of freshwater fishes with three species of *Henneguya* in Qena, Upper Egypt. Egypt Acad J Biol Sci 1:11–19

Rambaut A (2008) FigTree v1.1.1: Tree figure drawing tool. Available from: http://tree.bio.ed.ac.uk/software/figtree/

Resende EK (2003) Migratory fishes of the Paraguay-Paraná Basin excluding the upper Paraná Basin. In: Carolsfeld J, Harvey B, Ross C, Baer A (eds) Migratory fishes of South America: biology, fisheries and conservation status. World Fisheries Trust, The World Bank, and International Development Research Center, Ottawa, p 99

Editorial responsibility: Sven Klimpel, Frankfurt, Germany

Submitted: May 6, 2013; Accepted: October 15, 2013
Proofs received from author(s): December 19, 2013